Vortical flow structures at a helicopter rotor model measured by LDV and PIV

M. Raffel, U. Seelhorst† and C. Willert‡

Institut für Strömungsmechanik
Deutsches Zentrum für Luft- und Raumfahrt e.V. (DLR)
Bunsenstraße 10, Göttingen, Germany

ABSTRACT

Flowfield measurements of the blade tip vortices from a rotating helicopter rotor model were performed by three component laser-Doppler velocimetry (3D-LDV) and conventional (two component) particle image velocimetry (PIV). In general, the results are in good correspondence, but also illustrate the different properties of both techniques: LDV offers the capability of three-component measurements, whereas PIV captures the unsteadyness of the flowfield.

1.0 INTRODUCTION

With increasing use of civil helicopters the problem of noise emission of helicopters has become increasingly important within the last decades. Helicopter noise has been the subject of many research projects[1]. Blade vortex interactions (BVI) have been identified as a major source of impulsive noise. As BVI-noise is governed by the induced velocities of tip vortices, it depends on vortex strength and miss-distance, which itself depends on vortex location, orientation, and convection speed relative to the path of the advancing blade. Blade vortex interaction can occur at different locations inside the rotor plane depending on flight velocity and orientation of the blade tip path plane. Two types of BVI can be distinguished, (1) the angle between leading edge of the blade and vortex axis is about 0°, and (2) interactions at angles different from 0°. The noise emission of parallel blade vortex interaction is considerably larger[2, 3] compared to other cases of interaction. Investigations of the accoustic near and farfield[4, 5] were based on the interaction of the blade with vortices, which were described by mathematical models. Information about the structure and strength of the real rotor tip vortices and their interaction with the blade were not available. It is understood, that the study of these phenomena is of particular interest in progress towards quieter helicopters.

In our investigations the vortical structures of the flowfield of a helicopter rotor model in a windtunnel has been studied by optical measurement techniques, as only non-intrusive techniques are capable of obtaining velocity data within the rotor plane. Measurements of local flow vectors at positions close to the rotor blade tips were performed by three component laser Doppler velocimetry (3D-LDV) and conventional (two component) particle image velocimetry (PIV). LDV measurements on helicopter rotor models have intensively been performed over the past two decades[6-8]. The technique in general is described well in aerodynamic applications literature[9-11]. The application of PIV to high speed air flows started approximately ten years ago[12, 13]. Descriptions of multiple aerodynamic applications are given by Refs 14 and 15. PIV measurements on helicopter rotor models have been reported by Ref. 16. For the first time a comparison of LDV and PIV data acquired in a windtunnel from the same rotor model has been performed. The blade position has to be chosen where vortex positions and their orthogonal interactions with the blade are well known and easily reproducible.

2.0 ROTOR AND TEST MATRIX

The LDV and PIV measurements have been performed on the helicopter rotor model of the Department of Aerospace Engineering (ILR) of the Technical University RWTH Aachen, developed and instestigated in detail by Ref. 17 (see also Fig. 1 and 2). The rotor model had a radius of 0·5 m and four NACA 0015 blades (chord length = 54 mm) with rectangular tips. The rotor was driven by a toothed belt and an electric 65 kW engine and was fully articulated. It was installed in the open test section of the ILR Aachen low-speed windtunnel.

The freestream velocity was set to $U = 15\cdot7$ ms⁻¹ and the rotor speed to $f = 25$ rev/s resulting in an advance ratio of $\mu \approx 0\cdot2$. The tip path plane was tilted by an angle of $\alpha_{TPP} = -3°$ against the mean flow (forward flight), the collective part of the angle-of-attack was $\upsilon_{coll} = 10°$, and the cyclic pitch was $\upsilon_{cycl} = \pm3\cdot5°$ resulting in a trimmed condition. The Reynolds number, based on the blade chord length and blade tip velocity, was Re ≈ 278 000.

For the investigation of the blade tip vortex itself, 3D-LDV measurements have been performed at an azimuth angle of $\psi \approx 0°$ in a plane outside the rotor (Fig. 3, position A). At this position the blade tip vortex, generated at $\psi = 0°$, is about 3 ms old and has rolled up completely so that there is no temporal change in the vortex structure itself. The blade load, and therefore the vortex strength at this azimutal position is similar to that at $\psi = 90°$.

For the investigation of orthogonal blade vortex interaction LDV and PIV measurements have been taken at an azimuth angle of $\psi \approx 90°$ (advancing blade side) in a plane perpendicular to the freestream velocity (Fig. 3, position B).
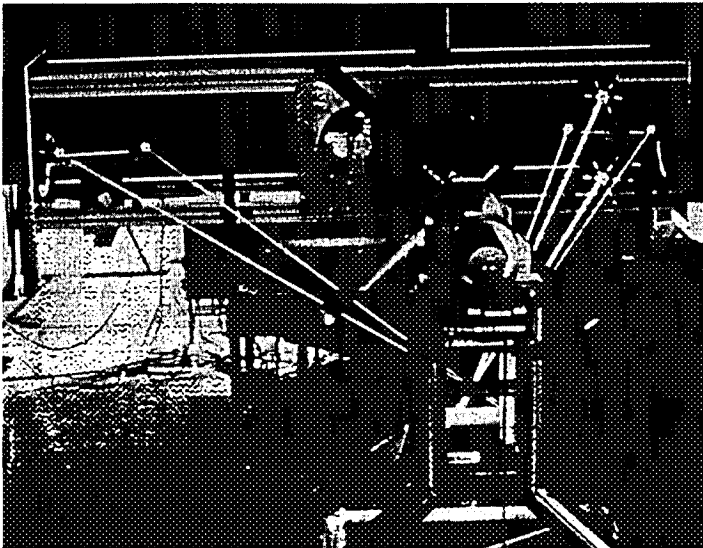
Figure 1. 3D–LDV and helicopter rotor model in the open test section of the ILR Aachen low-speed windtunnel.

3.0 3D-LDV SET-UP

The 3D-LDV system of the DLR Institute for Fluid Mechanics was operated in a back scatter, off-axis mode[18]. A 6 Watt argon-ion laser was used as a light source of which the three most intensive laser lines (476·5 nm, 488 nm, 514·5 nm) were utilised to distinguish the different velocity components (Fig. 4). Each of the laser beams was divided into two individual beams with similar intensity, one of which was superimposed with a Bragg shift of 40 Mhz to reduce ambiguity. The beams were coupled into single mode glass fibres and were launched into the probe volume with individual transmitting optics. In order to provide a good resolution of all three velocity components, the angle between the optical axes was set to 30°. The effective size of the probe volume was approximately 0·25 mm in diameter and 1 mm in length. The tracer particles used were the same for both the LDV and PIV measurements: oil droplets, with an average diameter of less than 1 μm. As the receiving optics of the
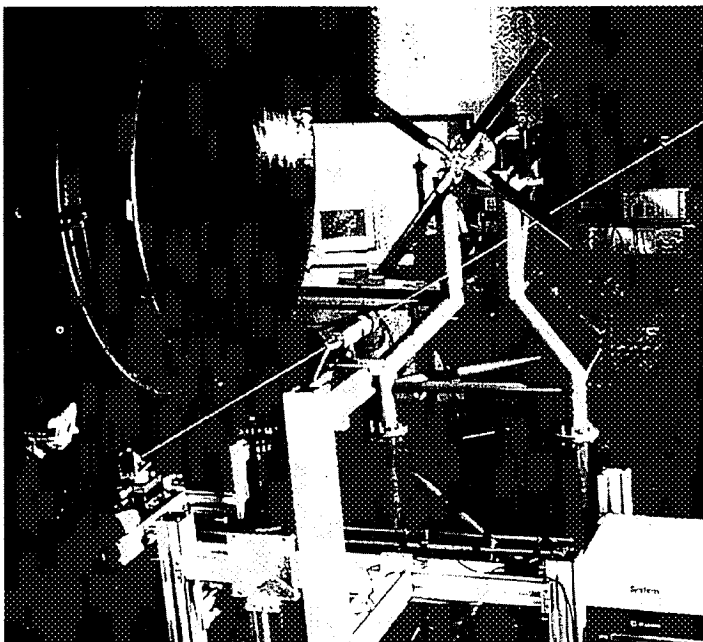

Figure 2. PIV set-up and helicopter rotor model in the open test section of the ILR Aachen low-speed windtunnel.
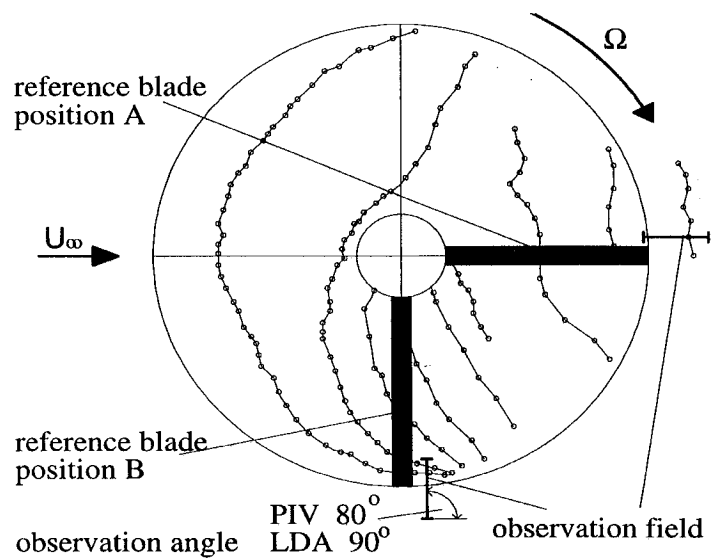

Figure 3. Sketch of the paths of the tip vortices at an advance ratio of (μ = 0·2, viewing direction parallel to the rotor axis, according to Beesten[17] — not to scale.

system operated in back-scatter mode, a sufficiently high data rate required the f-number of the receiving optics to be as small as possible. In this case a modified Schmidt-Cassegrain telescope with an aperture of 350 mm (f = 12) was used in order to gather sufficient scattered light from the particles. The received light, containing information of all three velocity components, was coupled into a multi-mode glass fibre, which transmited the light to a prism system in order to separate the different wavelengths. Then the light was converted into an electrical signal by three separate photo-multipliers.

After digitisation of the signals, a fast Fourier analysis yielded the desired Doppler frequency. Only if the signals of the three components coincided, was the velocity data stored together with the actual time and measuring position.

Based on the assumption of a periodic flowfield with respect to the rotor revolution, conditional sampling was used to get time dependent information of the flowfield. A trigger signal from the rotor axis was shifted with a time delay to any preselected azimuthal position of the rotor blade with an accuracy of 0·3% with respect to the rotor revolution. At this position, the data acquisition system clock was set to zero. Data acquisition was then started for a time window, corresponding to an azimuthal window or a time interval needed for the flow structure to pass through the probe volume. Usually data were acquired just within a small azimuthal window of 20° to 60°.

Converting time information into spatial information can be done in different ways. In this case the transformation of the time information into an equivalent azimuthal angle was done by the following equation
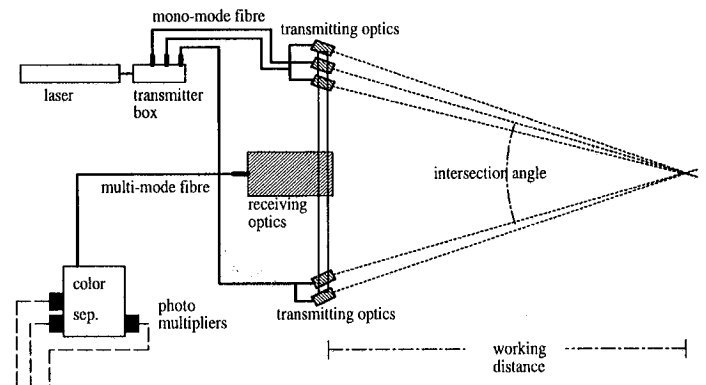

Figure 4. Sketch of the 3D-LDV system.

$\Psi = \Psi_0 + 2\pi \cdot f \cdot t$, where f is the rotor frequency   ... (1)

The transformation of the time dependent information into a spatial information of the flow structure as for example the length l was done by analysing the convection speed of the flow structure

$l = U_{conv} \cdot t$ ... (2)

Using the conditional sampling mode to acquire time resolved velocity data, which is later converted into spatial velocity data, leads to an inaccuracy due to the fact that flow structures may change during the time interval t, corresponding to the equivalent azimuthal angle. This has to be balanced against the significant reduction in measuring time.

The LDV signals were typically analysed with 128 samples per burst, resulting in a frequency resolution of approximately 0·1%. Based on the performance data, and the geometry of the setup used, the measurement uncertainty has been estimated to be approximately 0·3 ms⁻¹ for the velocity components normal to the axis of the receiving optics and 0·75 ms⁻¹ for the component parallel to the axis. An additional error due to the velocity lag of the tracer particles has to be taken into account. This problem is discussed intensively in literature[19, 20]. However, in the case of the particles used for the LDV and PIV measurements — 1 µm or less in diameter — the velocity lag can be said to be sufficiently small with respect to other measurement uncertainties[21] to be neglected.

A 'position monitoring system' gave access to blade motion parameters (lead-lag motion, pitching motion and angle of incidence) at a preselected radial position of the blade.

4.0 PIV RECORDING SYSTEM

During the last decade, PIV has increasingly been used to measure instantaneous flow velocity fields. This technique, in contrast to LDV, requires no conditional sampling. PIV allows the capture of the flow velocity in a two-dimensional plane within the flow within a few microseconds. It therefore allows for the entire velocity field to be obtained even in case of large cycle-to-cycle variations. The fact that the recording time necessary for the application of PIV (≈ 12 µs) is small compared to the time required for one revolution cycle (40 000 µs), makes PIV an ideal tool for the investigation of the unsteady flowfields associated with rotor aerodynamics.

During the past decade, a PIV system has been developed at DLR which can be operated under the rough environmental conditions in windtunnels[22]. This system utilises a dual-oscillator Nd:YAG pulse laser system with a maximum pulse energy of 2 × 70 mJ for illumination of an area of up to 20 × 30 cm² of the flowfield. The recordings are taken with a 35 mm photographic camera and are analysed by a fully digital evaluation system. The cross-correlation software[23] was used to recover the displacement data. During acquisition, the laser power was limited to approximately 60 mJ per pulse which was insufficient to saturate the sensor and produce adequately sized particle images; many particle images thus only covered 1-2 pixels. As a result the measurement uncertainty was of the order of pm 0·1 pixel. The maximum displacements were limited to less than 3 pixels around the strongest vortex due to the short pulse delay of 12 µs. As a consequence, the measurement uncertainty was large compared to the measured displacements. Nevertheless, the velocity data uncertainty has been estimated to be below 0·5 ms⁻¹ for the measured in-plane components. As stated earlier, the tracer particles used were the same as for LDV.

Using the synchronisation scheme shown in Fig. 5, the recording of the PIV images could be performed phase locked with the motion of the helicopter rotor model. Therefore, cycle-to-cycle variations of the flowfield at the same azimuthal angle of the reference blade could be investigated by analysing up to 100 recordings, each of which contained over 2000 independent velocity vectors. However, only the two in-plane components of the velocity vectors could be
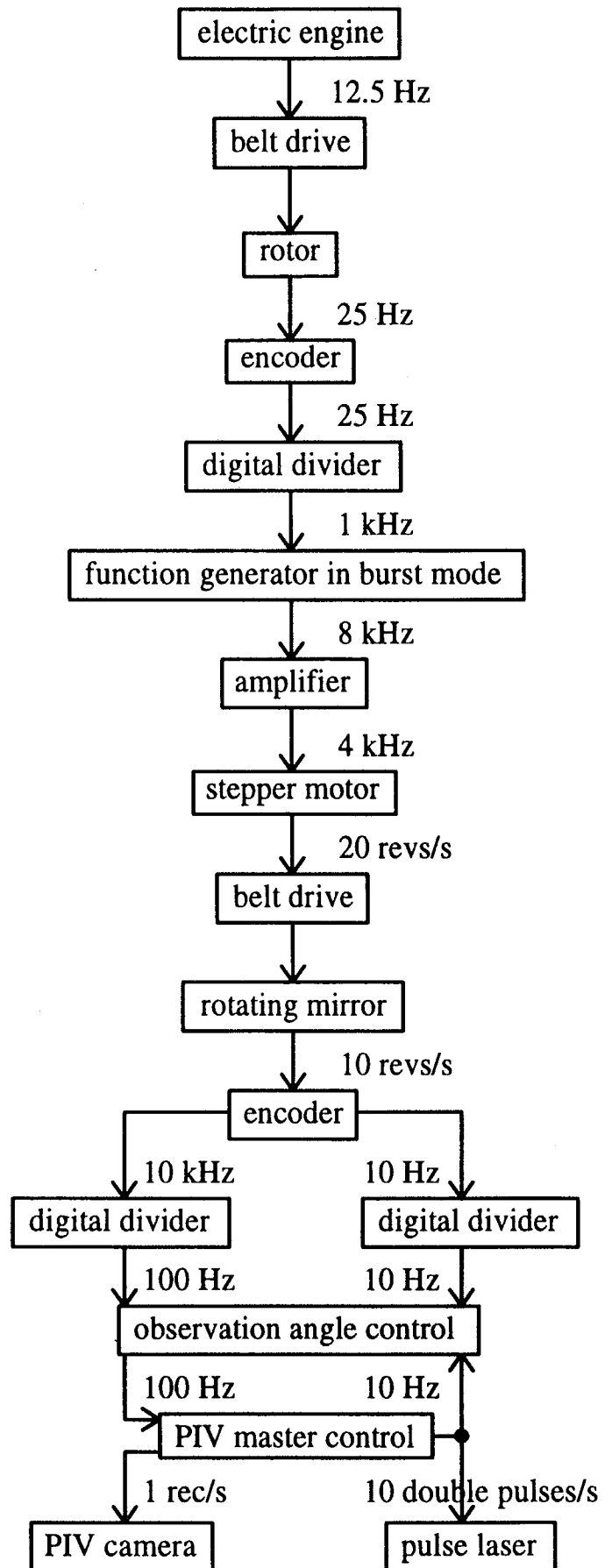

Figure 5. Synchronisation scheme of PIV data acquisition.

measured by means of the photographic PIV system. Examples of fully digital, non-photographic 2D-PIV measurements performed during the same measuring campaign are presented in Ref. 15.

5.0 LDV RESULTS

In Fig. 6 the tangential velocity profile of the tip vortex at $\psi = 0°$ is shown along a line through the vortex centre. For the measurement of the profile, the resolution was adapted to the extension of the vortex to be able to resolve the flowfield gradients. From this data the vortex core diameter has been estimated to be 4·8 mm, or 8·9 % of the blade chord respectivily, and a maximum tangential velocity of 18 ms⁻¹.

Figure 7 depicts the axial velocity profile of the tip vortex along the same line through the vortex centre as for the tangential velocity profile given in Fig. 6. For the axial velocity component, there is an increase in velocity of 4% to $W_{ax}/W_{tip} = 1·04$.

As shown in Fig. 3, LDV measurements in a conditional sampling mode were collected in a plane perpendicular to the freestream velocity at the advancing blade at an azimuthal angle of $\psi = 90°$. This yielded a three dimensional measurement grid, with the two coordinates obtained from traversing the LDV and the third coordinate derived from the transformation from time resolved velocity data to spatial velocity data. Associated with each of these grid points is a local three-dimensional velocity vector. By taking velocity data at each grid point for a time of 1·75 ms, corresponding to an angular window
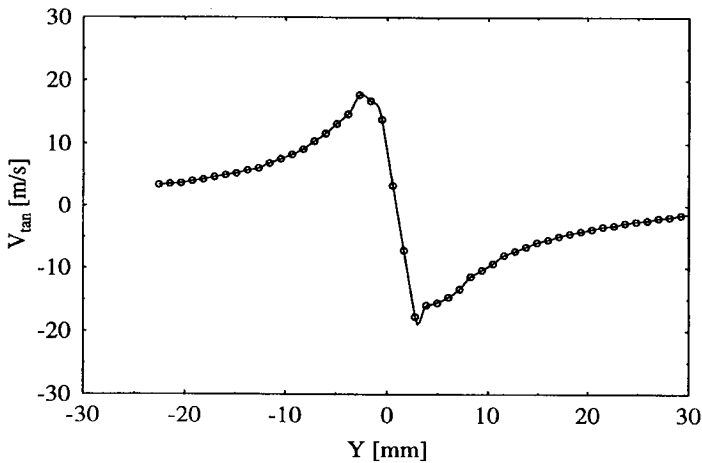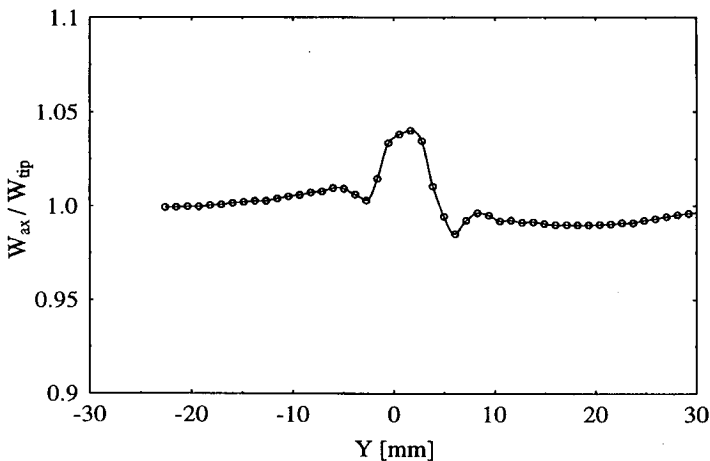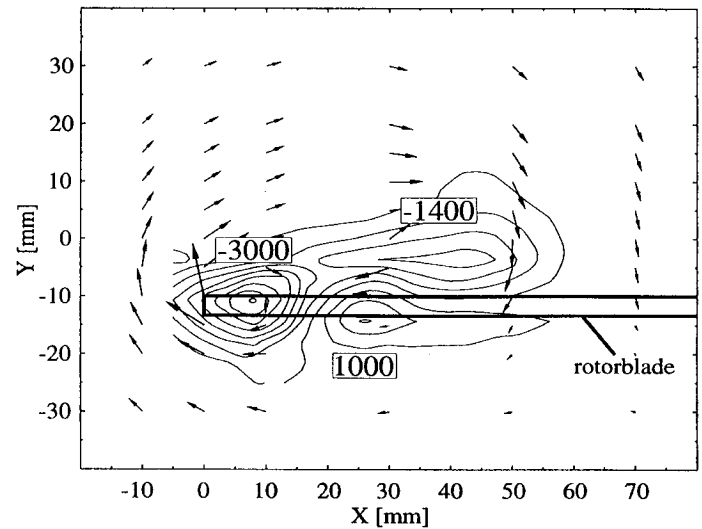

Figure 8. Velocity vector plot (2D) in a plane 0·2 chord length behind the blade tip as measured by LDV at $\psi = 90°$. The vorticity contours were obtained from the velocity data using finite differencing.
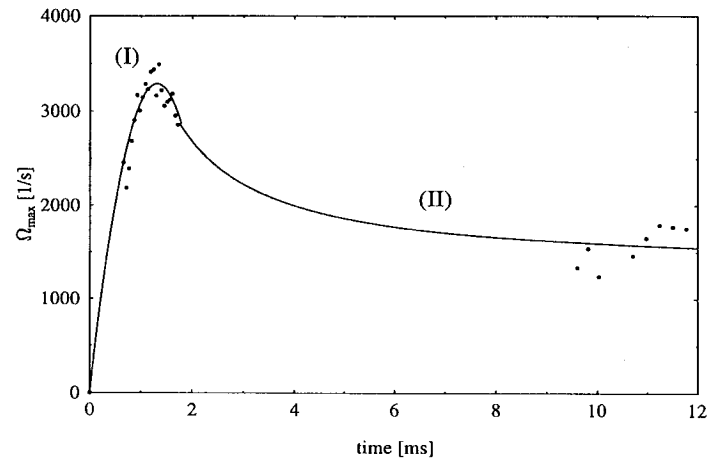
Figure 9. Temporal development of maximum vorticity of the blade tip vortex as measured by LDV at $\psi = 90°$.

of $\Delta\Psi = 10°$, leads, with a resolution of 0·5°, to a number of 20 measuring planes behind the rotor blade.

First, vector plots were computed from velocity data to give a general impression of the flow velocity field. Figure 8 shows the vortex locations inside the measurement grid. At this azimuthal position a vortex can be observed, which has just been generated (age = 0 ms, position corrected by the tip displacement $X = 7·5$ mm, $Y = 0$ mm). The vortex generated by the 90° preceeding blade (age = 10 ms, position corrected by the tip displacement $X = 43$ mm, $Y = 5$ mm) was located closer to the reference blade than expected (see also Fig. 10). Due to the location of the vortex generated by the advancing blade, an interaction with the blade occurs, which results in an additional vortex of opposite rotational direction ($X = 25$ mm, $Y = -5$ mm). Since the time between the generation of the tip vortices and their measurement is small (max 10 ms) the cycle-to-cycle variations can be expected to be small.

From each of the 20 planes, the maximum of vorticity of the newly generated blade tip vortex can be derived. This will give information on the temporal development. Due to conditional sampling, ten additional planes in advance of the rotor blade are also available, which includes information on the maximum vorticity of the vortex generated by the 90° preceeding blade. Figure 9 shows the temporal development of the maximum vorticity of the blade tip vortex from $t = 0$ ms


Figure 6. Tangential velocities along a line through the vortex centre obtained by 3D-LDV at $\psi = 0°$.

Figure 7. Axial velocities along a line through the vortex centre obtained by 3D-LDV at $\psi = 0°$.

up to $t = 12$ ms. The vortex formation (I) can be described by a second order polynominal, while its maximum vorticity decreases inversely proportional to its age, i.e. $1/t$ (II).

6.0 PIV RESULTS

PIV measurements of orthogonal blade vortex interaction (position B) were taken at an azimuthal angle of $\psi = 90°$, again on the advancing blade side. The observation area was nearly parallel to the trailing edge of the blade and orthogonal to the axis of the vortices. Figures 10(a) and (b) show two different instantaneous velocity vector fields from a set of 100 PIV recordings obtained at this angle. The origin was fixed to the tip of the trailing edge of the blade as it passed through the image plane with full aerodynamic load. Figure 10(c) is the velocity field obtained by averaging all 100 PIV data sets, and below (Fig. 10(d)) an estimate for the mean out-of-plane vorticity component is given. The tip vortex (A), which has just been generated (age ≈ 0 ms), was located at $X = 7.5$ mm, $Y = 2.5$ mm. A tip vortex (B), previously generated by the 90° preceeding blade (age ≈ 10 ms), is now located at $X = 22$ mm, $Y = 25$ mm.

The cycle-to-cycle variations of these two vortices were small enough such that they are properly resolved in the average velocity field. Close inspection of Figs 10(a) and (b) does, however, show some variations in the shape of the vortices. Also, a third vortex structure (C), generated by the 180° advancing blade, can be observed. As this vortex intersects the rotor plane, at the same time the blade intersects the image plane, it is sliced by the blade (i.e. orthogonal BVI) such that only its remnants can be observed in the velocity field of Fig. 10.

Due to small cycle-to-cycle variations, this third vortex is sliced differently each time, which results in the structure essentially being lost in the averaged velocity field (Fig. 10(c)).

In Fig. 11 the tangential velocity profile of a tip vortex (age ≈ 0 ms) from a single PIV velocity data set has been plotted along a line through the vortex centre.

From these data, the vortex core diameter has been estimated to be 7.4% of the blade chord at $\psi \approx 90°$, compared to 8.9% by the LDV method measured at $\psi \approx 0°$. The maximum tangential velocities (± 24 ms^{-1}) are 30% higher than those obtained by LDV (± 18 ms^{-1}). Also, it can be seen from the velocity profile in Fig. 11, that the V-component of the measured velocity does not converge to zero at the outer edges of the observation area. Similar results were recently presented by Ref. 16. This effect, and the discrepancy between the velocity profiles shown in Figs 6 and 11, can be explained by the fact that the flowfield measured at $\psi \approx 90°$, consists of different vortices and their interaction with the shear layer generated by the rotor blades. This made the determination of circulation of distinct vortices and a fit to analytical vortex models difficult. This is also the reason why further analysis of the vortices is based on peak vorticity instead of circulation.

In order to investigate the uncertainty resulting from averaging the velocity field, the data of a number of instantaneous velocity vector fields (Fig. 10) have been averaged. This way, the amount of decreasing maximum tangential velocity and increasing vortex core size due to the averaging process can also be determined.

Figure 12 shows the tangential velocity profile along a line through the vortex centre obtained by a spatial average over 36 PIV recordings. The maximum tangential velocity has been estimated to be ± 19 ms^{-1} and the vortex core size is 10.1% of the blade chord, both in good agreement with the LDV data. The maximum tangential velocity and the vortex core size are in the range of the results derived from the LDV data.

In analogy to the available LDV data, the calculation of the temporal development of the maximum vorticity for the newly generated tip vortex can be performed. In this regard PIV recordings were obtained at different azimuthal positions of the rotor blade. From these the maximum vorticity in relation to the rotor azimuth was derived.
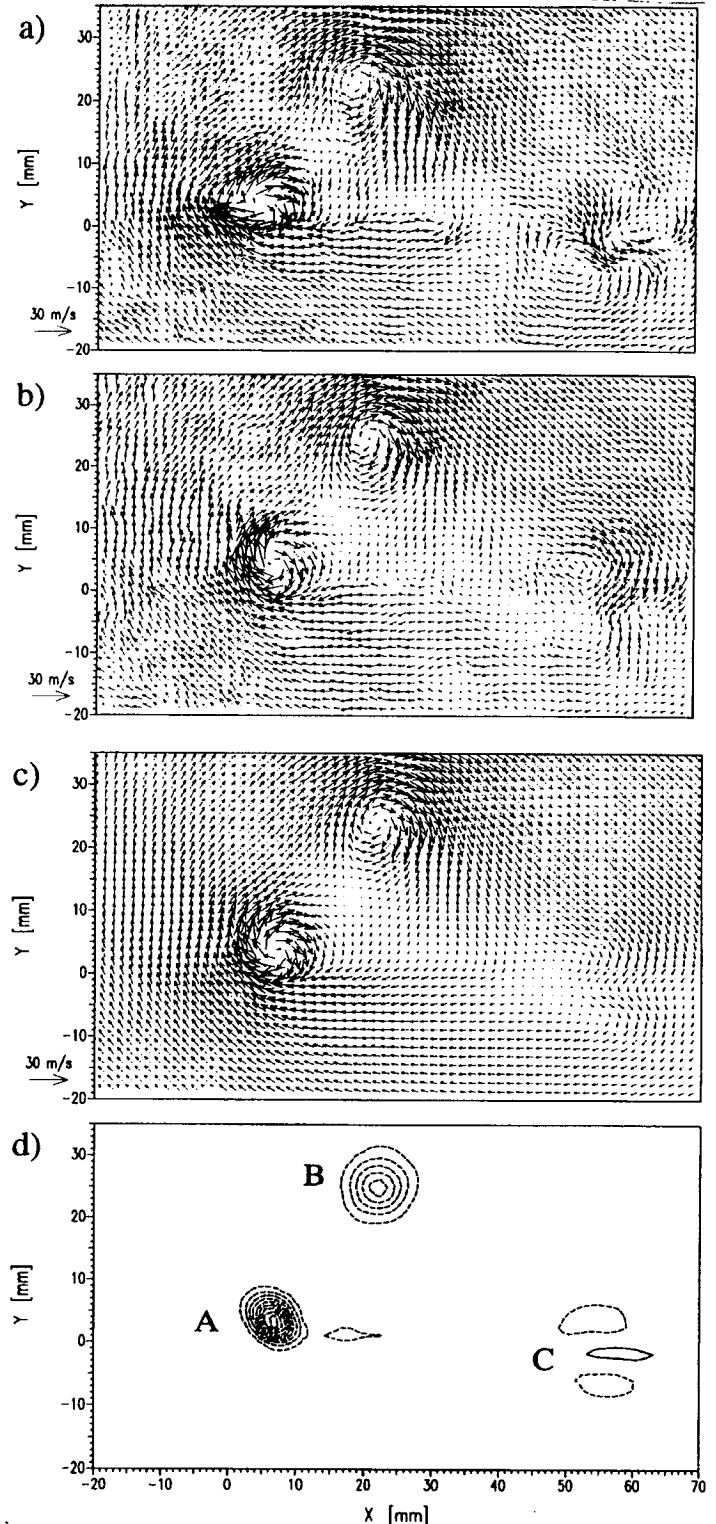

Figure 10. Two examples (a, b) of 100 instantaneous velocity vector fields as obtained by PIV at $\psi \approx 90°$. Below the averaged velocity field (c) and (d) the corresponding vorticity estimate, ω_z, is shown. (Contour levels are spaced at 400/s; dashed contours indicate negative values). Only portions of the 210 mm by 150 mm fields are shown for clarity.

As with the results derived from the LDV mesurements, the roll up process can be described by a second order polynominal, while the vortex dissipation is governed again by a 1/t dependence.

7.0 DISCUSSION

The 3D-LDV measurements yielded fundamental results concerning the structure of the blade tip vortices. In addition to geometric parameters like location of the vortex relative to the rotor plane and orientation of the vortex axis in space, the vortex core size, axial velocity, vortex strength, and vorticity distribution could be derived . Although blade motion and local velocity had been measured simultaneously, phase averaging and the rearrangement of the pointwise measured velocity data to form a complete velocity field causes some problems. Aperiodic flow phenomena, even of small amplitudes, can lead to the loss of information about the cycle-to-cycle variation resulting in an underestimate of the actual vortex strength, and an overestimate of the vortex core size.

However, recent LDV measurements in large aerodynamic facilities show that 3D-LDV data of high quality can be obtained with good spatial resolution[24].

In spite of the difficult experimental conditions, high quality PIV data were obtained with sufficient spatial resolution. The time needed for data acquisition can be considerably decreased compared to the LDV measurements. A specially developed synchronisation scheme allowed the capture of instantaneous flowfield measurements at exactly the same phase angle of the rotor revolution and therefore the study of aperiodic features of the flow. Also with PIV, the location of the vortex relative to the rotor plane, vortex core radius, convection speed and vorticity could be measured. However, since conventional PIV measures only two velocity components, data, like the orientation of the vortex axis in space and axial velocity of a vortex, cannot be derived without changing the viewing direction. The use of a second camera in a stereoscopic arrangement would allow the measurement of all three velocity components without averaging data of different cycles.

From the comparison between the LDV and PIV data, the differences in averaging and instantaneous data acquisition can be illustrated. By averaging a number of instantaneous PIV velocity vector maps, similar results to the LDA results are obtained, especially regarding the vortex core size and the maximum tangential velocity. The temporal development of vortex formation and its dissipation can be obtained from both the LDV and PIV results.

Future investigations should be performed by instantaneous measurements of the three velocity components e.g. by stereoscopic PIV, which has already been used in aerodynamic research[25, 26]. By
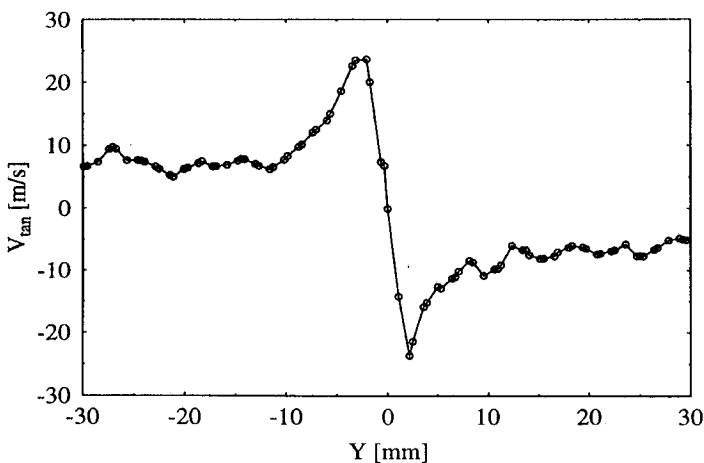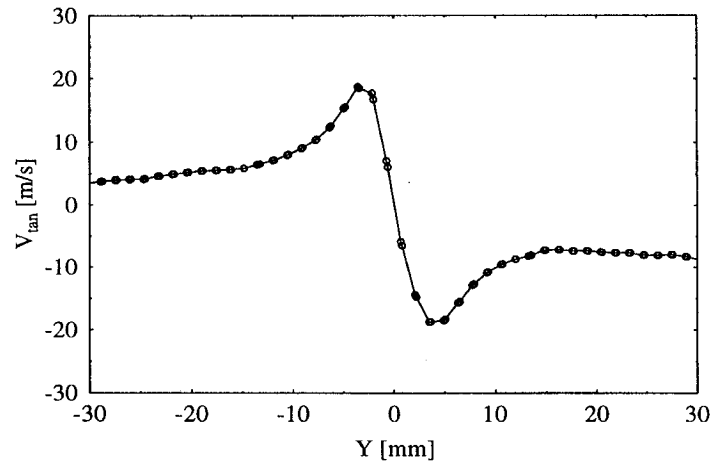

Figure 12. Tangential velocitiy along a line through the vortex centre as obtained by an average over 36 PIV recordings at $\psi \approx 90°$.
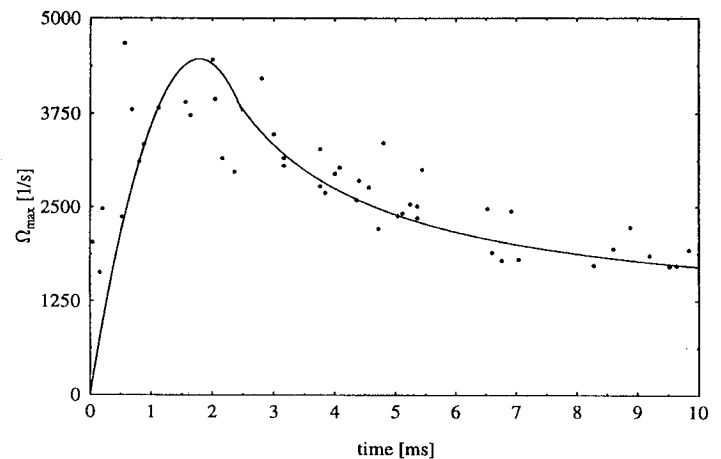

Figure 13. Temporal development of maximum vorticity of the blade tip vortex as measured by PIV at $\psi \approx 90°$.

the measurement of multiple parallel planes, more information about the orientation of the vortices axes can be obtained. More detailed studies of tip vortices from stationary blades and their interaction with blades[27, 28], should be performed in order to reduce the complexity of the vortical structures under investigation.

ACKNOWLEDGEMENT

REFERENCES

1. LOWSON, M.V. Progress towards quieter civil helicopters, Proc of the 17th European Rotorcraft Forum, Paper 59, Berlin, Germany 1991.
2. CARDONNE, F.X., LAUTENSCHLÄGER, J.L. and SILVA, M.J. An experimental study of rotor–vortex interaction, AIAA 88-0045, Aerospace Science Meeting, Reno, USA 1988.
3. SPLETTSTÖSSER, W.R., SCHULTZ, K.J. and MARTIN, R.M. Rotor blade-vortex interaction impulsive noise source localisation, AIAA J, 1990, 28, (4), pp 593-600.

Figure 11. Tangential velocitiy along a line through the vortex centre as obtained by a single PIV recording at $\psi \approx 90°$.

4.   EHRENFRIED, K., MEIER, G.E.A. and OBERMEIER, F. Sound produced by vortex-airfoil interaction, Proc of the 17th European Rotorcraft Forum, Paper 63, Berlin, Germany 1991.

5.   BURLEY, C.L., JONES, H.E., MARCOLINI, M.A. and SPLETTSTÖSSER, W.R. Directivity and prediction of low frequency rotor noise, AIAA 91-0592, Aerospace Science Meeting, Reno, USA 1991.

6.   BIGGERS, J.C. and ORLOFF, K.L. Laser velocimeter measurements of the helicopter rotor induced flowfield, 30th Annual National Forum of the American Helicopter Society, reprint No 800, May 1974.

7.   SULLIVAN, J.P. An experimental investigation of vortex rings and heli-copter rotor wakes using a laser Doppler velocimeter, MIT Technical Report 183, June 1973.

8.   ELLIOT, J.W., ALTHOFF, S.L., SELLERS, W.L. and NICHOLS, C.E. Inflow velocity measurements made on a helicopter rotor using two-component laser velocimeter, AIAA 19th Fluid Dynamics, Plasma Dynamics, and Laser Conference, Honolulu, Hawaii, AIAA, Paper 87-1321, June 1987.

9.   DURST, F., MELLING, A. and WHITELAW, H. *Principles and Practice of Laser Doppler Anemometry*, Academic Press, 1981

10. BOUTIER, A., PAGAN, D. and SOULEVANT, D. Measurement accuracy with 3D laser Velocimetry, Int Conf on Laser Application, Manchester, December 1985.

11. BÜTEFISCH, K.A. Three component laser Doppler anemometry in large windtunnels, *Prog Aerospace Sci*, 1989, **26**, pp 79-113.

12. KOMPENHANS, J. and HÖCKER, R. Application of particle image velocimetry to high speed flows, Von Karman Institute for Fluid Dynamics, Lecture Series 1988-06, Particle Image Displacement Velocimetry, Brussels, 21-25 March 1988, pp 67-83.

13. TOWERS, C.E., BRYANSTON-CROSS, P.J. and JUDGE, T.R. Application of particle image velocimetry to large-scale transonic windtunnels, *Optics & Laser Technology*, 1991, **23**, (5), pp 289-295.

14. HUMPHREYS, W.M., BARTRAM, S.M. and BLACKSHIRE, J.L. A survey of particle image velocimetry applications in Langley Aerospace facilities, 31st Aerospace Sciences Meeting, 11-14 January 1993, Reno, AIAA, Paper 93-041.

15. WILLERT, C.E., RAFFEL, M., STASICKI, B. and KOMPENHANS, J. High-speed digital video camera systems and related software for application of PIV in windtunnel flows, 8th Int Sym on Appl of Laser Techniques to Fluid Mech, Lisbon, Portugal, 1996.

16. MURASHIGE, A., TSUCHIHASHI, A., TSUJIUCHI, T. and YAMAKAWA, E. Blade-tip vortex measurement by PIV, Proc of the 23th European Rotorcraft Forum, Paper 36, Dresden, Germany, 1997.

17. BEESTEN, B.M.J. Nichtplanare Rotorblattspitzen im Hubschraubervor-wärtsflug, Doctoral thesis, RWTH-Aachen, 1994.

18. SEELHORST, U., BÜTEFISCH, K.A. and SAUERLAND, K.H. Three component laser Doppler velocimeter development for large windtun-nels, ICIASF 1993 Record, Paper 33, Saint Louis, France, 1993.

19. MELLING, A. Seeding gas flows for laser anemometry, AGARD Confer-ence on Advanced Instrumentation for Aero Engine Components, Philadelphia, 19-23 May 1986, AGARD-CP 399, Paper no 8.

20. MEYERS, J.F. Generation of particles and seeding, Von Karman Inst for Fluid Dynamics, Lecture Series 1991-05, Laser Velocimetry, Brussels, 10-14 June 1991.

21. HUNTER W.W. and NICHOLS, C.E. (Eds) Windtunnel seeding systems for laser velocimeters, Nasa Conf, (2393), Workshop, 19-20 March 1985, Nasa Langley Research Center.

22. KOMPENHANS, J., RAFFEL, M., VOGT, A., FISCHER, M., BRETTHAUER, B., VOLLMERS, H. and STASICKI, B. Investigation of unsteady flowfields in windtunnels at high flow velocities by means of particle image velocimetry, Proc of the 2nd International Conference on Experimental Fluid Mechanics ICEFM, ONORATO, M. (Ed) Levrotto and Bella, Turin, Italy 1994, pp 90-102.

23. WILLERT, C.E. The fully digital evaluation of photographic PIV recordings, Applied Scientific Research, 1995.

24. SPLETTSTÖSSER, W.R., KUBE, R., WAGNER,W., SEELHORST, U., BOUTIER, A., MICHELI, F. and MERCKER, E. Key results from a higher harmonic control aeroacoustic rotor test (HART) in the German-Dutch windtunnel, Proc of the 21th European Rotorcraft Forum, St Petersburg, Russia, 1995.

25. BEARMAN, P.W, HARVEY, J.K. and STEWART, J.N. Development of PIV for two and three component velocity measurements in a large low speed windtunnel, Proc of the 81th Meeting and Symposium of the Fluid Dynamics Panel (formerly AGARD) on Advanced Aerodynamic Measurement Technology, Seattle, USA, 1997.

26. WILLERT, C.E. Stereoscopic digital particle image velocimetry for applica-tion in windtunnel flows, accepted for publication in the special issue on particle image velocimetry of measurement, science, and technology, 1997.

27. HORNER, M.B., STEWART, J.N., GALBRAITH, R.A.McD., GRANT, I., COTON, F.N. and SMITH, G.H. Preliminary results from a particle image velocimetry study of blade-vortex interaction, *Aeronaut J*, March 1995, **99**, (983), pp 91-98.

28. HORNER, M.B. GALBRAITH, R.A.McD., COTON, F.N., STEWART, J.N. and GRANT, I. Examination of deformation during blade-vortex interaction, *AIAA J*, 1996, **34**, (6), pp 1188-1194.